

Sub-pixel mapping of tree canopy, impervious surface, and cropland in the Laurentian Great Lakes Basin using MODIS time-series data

Yang Shao and Ross S. Lunetta

Abstract— This research examined sub-pixel land-cover classification performance for tree canopy, impervious surface, and cropland in the Laurentian Great Lakes Basin (GLB) using both time-series MODIS (Moderate Resolution Imaging Spectroradiometer) NDVI (Normalized Difference Vegetation Index) and surface reflectance data. Classification training strategies included both an entire-region approach and an ecoregion-stratified approach, using multi-layer perceptron neural network classifiers. Although large variations in classification performances were observed for different ecoregions, the ecoregion-stratified approach did not significantly improve classification accuracies. Sub-pixel classification performances were largely dependent on different types of MODIS input datasets. Overall, the combination of MODIS surface reflectance bands 1–7 generated the best sub-pixel estimations of tree canopy ($R^2 = 0.57$), impervious surface ($R^2 = 0.63$) and cropland ($R^2 = 0.30$), which are considerable higher than those derived using only MODIS-NDVI data (tree canopy $R^2 = 0.50$, impervious surface $R^2 = 0.51$, and cropland $R^2 = 0.24$). Also, sub-pixel classification accuracies were much improved when the results were aggregated from 250 m to 500 m spatial resolution. The use of individual date MODIS images were also examined with the best results being achieved for Julian days 185 (early-July), 217 (early-August), and 113 (late-April) for tree canopy, impervious surface, and cropland, respectively. The results suggested the relative importance of the image data input selection, spatial resolution, and acquisition dates for the sub-pixel mapping of major cover types in the GLB.

Manuscript received November 5, 2009; revised February 23, 2010. This research was supported by EPA's Global Earth Observation System of Systems (GEOSS) under the Advanced Monitoring Initiative (AMI), Project No. 07-35. The United States Environmental Protection Agency (EPA) funded and conducted the research described in this paper. Although this work was reviewed by EPA and has been approved for publication, it may not necessarily reflect official Agency policy. Mention of any trade names or commercial products does not constitute endorsement or recommendation for use.

Yang Shao is with the U.S. Environmental Protection Agency, National Research Council, National Exposure Research Laboratory, 109 T.W. Alexander Drive, Research Triangle Park, NC 27711, USA (e-mail: shao.yang@epa.gov).

Ross S. Lunetta is with the U.S. Environmental Protection Agency, National Exposure Research Laboratory, 109 T.W. Alexander Drive, Research Triangle Park, NC 27711, USA (e-mail: lunetta.ross@epa.gov).

Index Terms— Land-Cover Mapping, Sub-Pixel Unmixing, Accuracy Assessment.

I. INTRODUCTION

Land-cover (LC) types, their distributions, and their dynamics are important landscape characteristics needed for the study of terrestrial ecosystem processes, climate change impacts, and human-environmental interactions [1-3]. Recently, the Moderate Resolution Imaging Spectroradiometer (MODIS) data has been increasingly used for regional and global LC mapping [4-6]. The moderate spatial resolution and high temporal resolution attributes are particularly important for many large-area mapping applications [7]. Currently, global and regional LC map products can be routinely generated at a range of 250 m to 1,000 m spatial resolution and researchers are developing maps and change detection products at 250 m resolution [5], [8-10].

Landscape patterns can often be heterogeneous and contain a complex mixture of cover types. A similar cover type (e.g., forest) may have variable spatial characteristics (i.e., sizes and shapes) across different geographic locations [11]. Consequently, LC mapping at regional scales is inherently difficult using remote sensing data with arbitrarily defined spectral, spatial, and temporal resolutions. The accuracy of global-regional LC products may vary substantially across different subregions due to the heterogeneity of cover type patterns. For example, accuracy levels for individual continents in the International Geosphere-Biosphere Programme (IGBP) global LC map product differed by as much as 20% [11]. Generally, classification accuracy decreases with increased heterogeneity and decreased patch size [12]. The LC mixture in moderate-coarse spatial resolution data presents a significant challenge for image classification, as well as accuracy assessment [13], [14].

One common solution for the mixture problem is to conduct spectral unmixing that estimates proportional cover types within each pixel. Intensive research has been conducted for sub-pixel composition estimates using Advanced Very High Resolution Radiometer (AVHRR) and MODIS data [15-17]. More recently research has focused on the development of a global percent tree canopy cover product using 500 m MODIS time-series data [5].

Similar to per-pixel mapping, the performance of sub-pixel

LC estimation may also vary across different areas or subregions, depending on cover type heterogeneity, imagery resolution, and analytical methods applied. A review of recent remote sensing literature suggests that sub-pixel classification accuracies are often reported for the entire area of interest [13]. As a result, spatial variations of classification quality at the subregional level are often poorly understood. This can lead to inconsistent map quality, which may lead to erroneous results in subsequent change analysis, environmental assessment, and other applications that incorporate LC products as primary inputs. Previous studies suggested that ecoregion-based image stratification may be used to reduce the complexity of the large-area mapping problem. Performing independent image categorizations within individual ecoregions may improve performance [18]. The ecoregion-based approaches, however, have not been fully examined for sub-pixel performance, especially for MODIS-derived products.

The performances of sub-pixel classification may also depend on the MODIS data type(s). MODIS NDVI (Normalized Difference Vegetation Index) and surface reflectance values are two commonly used inputs to the sub-pixel classifier [5], [19]. Some researchers may choose MODIS products from a single acquisition date for sub-pixel classification, while most have used time-series MODIS products such as the 8-day or 16-day composite data. In practice, few studies have quantified the differences of sub-pixel categorization performances using different MODIS products (e.g., NDVI and/or reflectance bands). Additionally, it is widely accepted that the use of time-series data may improve the classification performance compared to the use of an individual image; however, the magnitude of improvement has not been reported. Researchers have also derived phenometrics (i.e., start and end of season) from time-series data; however, the use of phenometrics for image classification can be questionable and lower classification accuracy might be obtained compared to the direct use of time-series data [20]. The primary concern of using time-series data is the increase in data dimensionality. The so-called “curse of dimensionality” problem may lead to slower training and even a deterioration in categorization performance [21]. The spatial registration problem in time-series datasets may also cause difficulties for sub-pixel classification with time-series data, including medium resolution MODIS data at 250 m [22].

A. Research Objectives

The goal of this study was to examine the potential of MODIS data for the sub-pixel LC classifications. The experimental design was developed to provide a better understanding of the interactions between spectral, spatial, and temporal resolutions for the purpose of the sub-pixel mapping. Three general cover types were considered included tree canopy, impervious surface, and cropland. Sub-pixel classification experiments were conducted for Laurentian Great Lakes Basin (GLB); which includes all or part of eight states within the US and a portion of the Province of Ontario,

Canada. The specific research objectives addressed in this study included the following (TABLE I).

(1) Examine the spatial variations of classification performances across different sub-regions of the GLB. Develop an ecoregion-based sub-pixel classification approach to quantify the differences in classification performances between an entire-region versus an ecoregion-stratified approach.

(2) Determine how the sub-pixel classification performance may vary when different MODIS input datasets are used. Two standard MODIS data products were examined: MODIS-NDVI and MODIS surface reflectance values. For MODIS surface reflectance data, a number of MODIS band combinations were tested for the sub-pixel classification.

(3) Compare the sub-pixel classification performances between MODIS time-series data and individual images.

B. Study Area

The GLB region includes all or part of eight states of the United States and a portion of the province of Ontario, Canada. The region spans more than 1,200 km from west to east, and it contains the largest surface freshwater system on the Earth. The southern portion of GLB is heavily industrialized. More than ten major metropolitan areas are located in the southern portion of the GLB. The highest density of croplands is located in the southern half of the GLB, especially in the states of Michigan, Ohio, and Wisconsin in the United States and the southern portion of Ontario. The northern portion of the GLB is relatively undeveloped. Climate and soil quality limit large-scale agriculture. It is dominated by diverse forest types, freshwater aquatic systems, and wetlands.

The major LC change in the GLB is believed to be urbanization from the last four decades [23]. Urban expansions occurred around edges of metropolitan areas and other smaller cities in both the United States and Canadian portions of the GLB, typically at the cost of agricultural lands [24]. Urban expansion and agricultural intensification in the GLB has caused increased concerns about water quality, natural habitats, and ecosystem health related issues [25], [26]. Currently, many remote sensing mapping efforts are being conducted by both the US and Canadian governmental agencies, but most have been focused on decadal data products (e.g., NLCD-2001). The lack of a consistent mapping approach and product schedule could negatively impact future GLB-wide environmental assessment efforts.

II. DATA AND PRE-PROCESSING

The 2001 National Land Cover Database (NLCD-2001) was obtained from the United States Geological Survey (USGS), Earth Resources Observation and Science (EROS) Data Center. In addition to the most commonly used 2001 LC thematic data, the impervious surface data and the tree canopy data were also acquired from EROS. All three datasets have 30 m spatial resolution. The fractional impervious surface and tree canopy were estimated for each 30 m pixel using regression tree techniques. The accuracies were estimated to

be about 83–91% and 78–93% for the impervious surface and tree canopy, respectively [27]. The finer spatial resolution (30 m) of the NLCD allowed us to develop proportional cover type maps at coarser spatial scale (e.g., 250 m), which can be used as reference dataset to examine the potential of MODIS sub-pixel classification.

MODIS time-series products from year 2001 were acquired from the USGS EROS Data Center. These included the 250 m 16-day NDVI composite data (MOD13Q1), 250 m 8-day surface reflectance composite data (MOD09Q1), and 500 m 8-day surface reflectance composite data (MOD09A1). The 250 m 8-day surface reflectance data include two spectral bands, centered at 648 nm (red) and 858 nm (NIR), respectively. The 500 m 8-day surface reflectance data provides seven spectral bands at 500 m resolution. In addition to red and NIR bands, the 500 m data also contains spectral bands centered at 470 nm, 555 nm, 1240 nm, 1640 nm, and 2130 nm.

The NLCD-2001 and MODIS data products were re-projected to an Alber's Equal Area Conic projection. For MODIS data products, a Savitzky–Golay filter was applied to estimate new values for pixels with poor quality control (QC) flags [28]. The spatial extents of snow cover were substantial for winter and early spring in the GLB, thus the MODIS time-series data products in those time-periods were discarded. MODIS datasets from Julian day-of-year (DOY) 97 (early-April) to 273 (late-September) were used as primary inputs to characterize sub-pixel LC information. There were also noticeable error observed for some water pixels in lakes and large streams. These pixels have extremely high NDVI values (e.g., >0.7). All water pixels in MODIS data thus were masked out using NLCD-2001 as references.

A geographic linkage between the NLCD-2001 and the MODIS products was developed. For each 250m MODIS pixel, cover type proportions were calculated for tree canopy, impervious surface, and cropland. For tree canopy and impervious surface, the NLCD-2001 continuous LC data were simply aggregated to 250 m scale. For cropland, the thematic cover type (class 82) was used as input for spatial aggregation. It was assumed that each 30 m NLCD cropland pixel was homogeneous.

III. METHODS

A. GLB versus Ecoregion Approach

Sub-pixel classifications were examined for two training strategies using time-series MODIS-NDVI data. The first strategy was the entire-region classification approach using training data points randomly selected from the entire US portion of the GLB. The second training strategy was to stratify the entire GLB into 12 ecoregions [29] to support an independent sub-pixel classification for each ecoregion (Fig. 1). New training sample set was randomly selected within each ecoregion boundary for the ecoregion-stratified classification. The motivation for the image stratification was to reduce the complexity associated with the large-area mapping problem, and potentially improve classification

performance.

A three layer multi-perceptron (MLP) neural network (NN) was employed for the sub-pixel classification. Although the regression tree is probably the most commonly used algorithm for large-area sub-pixel mapping problems, a number of recent studies suggested that MLP-NN regression may also achieve similar or higher sub-pixel classification accuracies, especially when appropriate training protocols are used [30], [31]. The UNIX-based Stuttgart Neural Network Simulator software package was used for the three layer MLP-NN training and classification. The three layer MLP-NN consisted of one input layer, one hidden layer, and one output layer. The number of nodes at the input layer depends on the number of input features. A total of 12 input features were used to represent MODIS-NDVI 16-day composite data obtained from Julian day 97 to 273. The number of hidden nodes typically needs to be examined through a trial-and-error approach in practice. There was only one output node at the output layer, representing sub-pixel LC estimation for each specific cover type (e.g., tree canopy). It should be noted that because three cover types were considered for sub-pixel classification, three independent NNs for the sub-pixel estimations of tree canopy, impervious surface, and cropland were required.

To train the NN regression, sub-pixel proportional data were required for the training pixels to provide output targets. The NN simply approximated the regression function between the input features (e.g., MODIS-NDVI) and the target values. For each NN classifier, only a small percentage (0.2%) of MODIS-NDVI pixels was selected for network training. The training data points were further divided into training and validation groups. It was important to have a validation dataset to reduce the risk of over-fitting and increased generalization [17], [21].

For the entire-region classification approach, the training sample size was 10,292 pixels. For the ecoregion-stratified approach, the training sample size ranged from 636 to 2,644 for different ecoregions. Several network training protocols such as learning rate, momentum, and the number of hidden layer nodes were examined to achieve optimal sub-pixel classification performance.

Generally, a higher learning rate (*i.e.*, 0.2) leads to faster network training; however, the network learning may tend to oscillate, thus causing unstable classification results [21]. On the other hand, a small learning rate (*i.e.*, 0.01) may result in long training time. For this study, three different learning rates (0.01, 0.05, and 0.1) were examined. The momentum was specified as 0.9 to reduce the risk of local minima. The numbers of nodes in the hidden layer were examined at 6, 12, and 24. For all NN classifiers, the training was stopped when the minimum error was achieved according to the validation dataset. It should be noted that the network training can be easily trapped in local minima, depending on the initial weights and learning protocol employed, therefore, network training were repeated 10 times for all parameter settings to obtain the best solution. The trained networks were then employed for the sub-pixel classification of the GLB.

B. NDVI and Reflectance Data

The MODIS-NDVI data products contain important information for vegetation-related applications; however, the NDVI may suffer data nonlinearity, scaling and signal saturation problems that could reduce its usefulness for sub-pixel LC mapping applications [6], [14]. Both the MODIS surface reflectance bands at 250 m and 500 m were also examined for the sub-pixel classification. The 500 m pixels from MODIS bands 3–7 (MOD09A1) were rescaled to 250 m to match the spatial resolutions in MODIS bands 1 and 2 (MOD09Q1). As with the MODIS-NDVI classification, the surface reflectance bands from DOY 97 to 273 were used as inputs for the sub-pixel classification.

One of the main concerns for using multiple MODIS surface reflectance data was the growing number of input data features. The 8-day composite surface reflectance data (e.g., DOY 97 to 273) have 26 composite images for each spectral band. The total number of input features could increase to 182 (26×7) if all seven MODIS spectral bands were used for the sub-pixel classification. The “curse of dimensionality” problem could increase computational requirements and possibly deteriorate classification performance [21]. Here we examined three simple band selection approaches. The first approach used MODIS bands 1 and 2 (red and NIR) as inputs, yielding a total of 52 (26×2) input features. In the second approach, the MODIS bands 1 and 2 were combined with one additional band from MODIS bands 3–7. The results for the five possible three-band combinations were compared, and the best band combinations were identified. The third approach used an “all-band” combination including MODIS bands 1–7, to make full use of the MODIS spectral signals. The same training data points were used for all the MODIS-NDVI and MODIS surface reflectance classifications, so the results could be directly compared for different inputs or MODIS band combinations.

C. Single Date versus Time-Series Data

The performance of individual MODIS images (e.g., DOY 105) within the composite time period was further examined for the estimation of sub-pixel unmixing. For example, there were 12 individual NDVI images for the MODIS-NDVI 16-day composite data from DOY 97 to 273. A total of 12 independent NN classifiers were developed for tree canopy estimations; each classifier used only one NDVI image as input for the sub-pixel classification. The same training data points were used as those for the entire time-series MODIS data classification. This allowed us to examine whether it is necessary to use the entire time-series data, or simply use the best individual image at a certain acquisition time for the sub-pixel classification. Additionally, comparing individual images may reveal their relative importance with respect to the sub-pixel cover type mapping.

D. Validation

Accuracy assessments were conducted for the entire United States portion of the GLB. The pixels used in the training and validation procedures were removed and all the remaining pixels were used to generate random data points (i.e., 2% of

total points) to support the accuracy assessments. There were no similar reference datasets available for the Canadian portion of the GLB, thus no assessments were conducted for Canada. Two statistical measures were used for the accuracy assessments: root-mean-square-error (RMSE) and the Pearson coefficient of determination (R^2). It should be noted that the RMSE and R^2 values may be disrupted if a large number of pixels with 0% and 100% fraction cover (i.e., pure pixels) are used in accuracy assessment [32]. In this study, we focused on the pixels with fraction cover (i.e., tree canopy) in the range of 5% to 95%, because these pixels can be considered as actual mixed pixels.

The results were reported for all three cover types (tree canopy, impervious surface, and cropland). Accuracy assessments were also conducted at 500 m resolution by simply scaling up the 250 m sub-pixel cover type fractions to reduce the impacts of mis-registration between MODIS and NLCD-2001 reference data.

IV. RESULTS AND DISCUSSION

A. GLB versus Ecoregion Approach

For the entire-region approach using MODIS-NDVI inputs, the RMSE values were 0.20, 0.18, and 0.29 for tree canopy, impervious surface, and cropland, respectively. Corresponding R^2 values were 0.50, 0.51 and 0.24, respectively. Because GLB is a relatively large and complex study region, large variations of sub-pixel classification performances were expected. TABLE II shows RMSE and R^2 values across the ten different ecoregions. For tree canopy, the R^2 values ranged from 0.19 to 0.50. The lowest R^2 were obtained for ecoregion 4, mainly located in the State of Ohio. Based on the NLCD-2001, this ecoregion was dominated (>63%) by cropland. Tree canopy only consisted of less than 8% of total land area. The NLCD-2001 also shows that forest fragmentation was higher in ecoregion 4 compared to other ecoregions [33]. Visual interpretation of the sub-pixel tree canopy estimates suggested that there were overestimations of tree canopy for a significant number of cropland pixels. A similar problem was reported by [27], although their research was based on a sub-pixel classification of Landsat data.

The R^2 values for impervious cover ranged from 0.19 to 0.61. The best estimation was obtained for ecoregion 10, where two major cities (Milwaukee and Chicago) are located. Relatively low R^2 values were obtained for ecoregions 2, 7, 8 and 9. Statistics from NLCD-2001 also suggested that there were relatively less urban area (i.e., <1%) in these ecoregions compared to other ecoregions (i.e., >2.5% urban area), and it was difficult to estimate small and scattered impervious patches using MODIS-NDVI data. Visual interpretation of sub-pixel impervious surface estimate indicated that there was obvious classification error for Michigan's Upper Peninsula or ecoregion 9, and a significant number of bare soil and cropland pixels were falsely estimated with over 30% impervious surface proportions. The spectral confusion between impervious surface, bare soil and cropland may cause the low sub-pixel classification accuracy [34]. The R^2 values for cropland ranged from 0.05 to 0.23, with the poorest result

being obtained for ecoregion 9, where the few cropland areas (2% estimated by the NLCD-2001) were sparsely distributed.

The large variation of sub-pixel classification accuracies across the GLB is a cause of concern for potential map users. Ecoregion-stratified sub-pixel classifications were conducted and the results were compared to those of the entire-region classification approach. Fig. 2 a-c compare R^2 values for the two approaches. For tree canopy, ecoregion-stratification improved sub-pixel classification results for ecoregions 4, 6, 7 and 10. In contrast, the entire-region classification approach generated similar or slightly higher sub-pixel classification performance for tree canopy in the remaining seven ecoregions. For impervious surface and cropland, there was also no clear advantage using the ecoregion-stratified approach. This result was unexpected, because the initial purpose of image stratification was to reduce the complexity of sub-pixel classification and thereby improve classification performance.

One possible reason for the lack of performance improvement using ecoregion-stratification approach was the limited number of training pixels used. In training the neural network, only a small number of training pixels (e.g., 0.2 %) were randomly selected. To determine if the training data provided insufficient information associated with sub-pixel variations for specific cover types (e.g., impervious surface), the percentage of training pixels was increased from 0.2% to 10% of the MODIS-NDVI pixels. The network training and classification were repeated for each individual ecoregion. The sub-pixel classification accuracies were assessed at both ecoregion and entire GLB scales. At individual ecoregion level, R^2 values for tree canopy increased approximately 1–4% for several ecoregions. The slight improvement was mainly observed for ecoregions with relatively lower tree canopy cover. Similar rates of improvement were also obtained for impervious surface and cropland. At the entire GLB scale, the R^2 values were 0.53, 0.52 and 0.25 for tree canopy, impervious surface and cropland, respectively. These values were only slightly better than those obtained from the entire-region sub-pixel classification approach.

B. NDVI and Surface Reflectance Analysis

TABLE III shows the RMSE and R^2 values calculated by using different MODIS input datasets for the sub-pixel classification. The results are reported for the entire-region classification approach only, because the ecoregion-stratified approach did not achieve higher classification accuracies. For tree canopy, the RMSE values (i.e., 0.19–0.20) were fairly close for different band selection scenarios. The use of MODIS surface reflectance bands 1 and 2 increased R^2 to 0.56 compared to MODIS-NDVI data ($R^2 = 0.50$). The addition of MODIS spectral bands from 3–7 and the MODIS all-band combination only achieved a slight increase of R^2 value. A possible reason is that because 8-day MODIS surface reflectance bands 1 and 2 already captured a majority of vegetation-related information, thus it provided the most efficient approach for sub-pixel tree canopy mapping.

The R^2 values for sub-pixel impervious surface were 0.51 and 0.57 by using MODIS-NDVI and MODIS surface

reflectance bands 1 and 2, respectively. The combination of MODIS bands 1, 2, and 6 further increased the R^2 to 0.59. It should be noted that all possible three-band combinations were examined. The combination of MODIS bands 1, 2, and 6 appeared to provide the best overall performance among all possible three band combinations. The MODIS all-band combination achieved the highest R^2 value (0.63), which was about 12 percent higher than using MODIS-NDVI as inputs. The RMSE value (0.15) obtained for the MODIS all-band combination was also much lower than the number derived for the MODIS-NDVI input (RMSE = 0.18). Visual comparison of sub-pixel classification maps suggested that the major factor contributing to the performance improvement was a reduction of confusion between impervious surface, cropland, and bare soil. For sub-pixel cropland estimation, the MODIS all-band combination also achieved the best overall performance (RMSE = 0.26, $R^2 = 0.30$). This represented a 6% (R^2) increase compared to the results for the 16-day MODIS-NDVI data.

Overall, MODIS-NDVI data performed poorest among the four scenarios tested for all three cover types (TABLE I and III). The computation of NDVI can be considered as a feature transformation procedure that reduces the spectral information contained in the original surface reflectance bands. This reduction in information may decrease the sub-pixel classification performances. In addition, the MODIS-NDVI data used in this study were 16-day composite products, which have a coarser temporal resolution than those of 8-day MODIS surface reflectance bands. The choice of a coarse composite time-period (i.e., 16 versus 8) might be beneficial for noise reduction purpose, but it may also lose crucial spectral information for cover type mapping. Generally, the sub-pixel classification performance improves when the number of MODIS surface reflectance bands increases. The impact of MODIS MIR bands for sub-pixel impervious cover mapping was particularly strong. The results were supported by studies using other remote sensing data for the urban and impervious mapping [35], [36]. Although there were concerns with the handling of multiple spatial resolutions (i.e., 500 m versus 250 m), the results suggested that it is still beneficial to examine data fusion or data stacking from multiple spatial scales. The comparison of different MODIS band combinations also indicated that “the curse of dimensionality” was not an issue for this sub-pixel mapping application, because the all-band combination performed best for both impervious cover and cropland mapping.

TABLE IV shows the accuracy statistics at 500 m spatial scale. The RMSE values reduced approximately 1–9% for different land cover types compared to those from the 250 m data. Consistent with that result, the R^2 values for the 500 m data were approximately 3–29% higher than for the 250 m data. Fig. 3 illustrates reduced scattering at 500 m for the three cover types compared to 250 m. The results from the MODIS all-band combination were used for the cross-plots and comparison. The sub-pixel classification accuracy

increased if pixels were scaled up to coarse spatial resolutions. These results were consistent with those previously reported [5]. The mis-registration between the NLCD-2001 and MODIS data might be reduced as coarser spatial scales were used as mapping units. The classification uncertainties or errors tend to smooth out as results were aggregated. In addition, MODIS's point spread function is along-scan tridiagonal and extends half pixel in the neighboring pixels [37], [38]. This may explain that the integration of sub-pixel estimation over a larger area yields better results. We further developed simple regression lines between the actual sub-pixel cover type proportions (i.e., NLCD-2001) and the estimated proportions from the MODIS data. At 250 m spatial scale, the slope values were 0.83, 0.86, and 0.73 for tree canopy, impervious surface, and cropland, respectively. The MODIS-based sub-pixel classification appeared to underestimate land cover proportions at the high extremes. The slope values increased to 0.95, 0.94, and 0.82 at the 500 m spatial scale. This further suggested the improved sub-pixel classification performance at coarse spatial resolutions. Fig. 4 shows the sub-pixel proportional maps for tree canopy, impervious surface, and cropland. Results were estimated by using MODIS all-band combination. Only a subset of the GLB study region was presented for better visual interpretability. The sub-pixel cover proportions were aggregated to five categories using 20% equal intervals, which clearly illustrate the different intensity levels of cover types.

C. Single Date versus Time-series Analysis

TABLE V(a) shows the highest R^2 values derived from individual images (or individual DOY) using MODIS-NDVI, MODIS bands 1 and 2, MODIS three-band combination, and MODIS all-band as inputs. For MODIS-NDVI data, the best results were obtained for images from DOY 193, DOY 209, and DOY 145 for tree canopy, impervious surface, and cropland, respectively. For all other band selection scenarios, the best results were obtained for images from DOY 185, DOY 217, and DOY 113 for three cover types, respectively. For tree canopy, the R^2 values were in the range of 0.38 to 0.46 using different MODIS input datasets. For impervious surface, the range of R^2 values was 0.45 to 0.60. For cropland, the range of R^2 values was 0.21 to 0.26. TABLE V(b) shows the R^2 values derived using entire time-series composite data from DOY 97 to 273 as inputs. The use of entire time-series of MODIS data largely increased R^2 values for tree canopy and impervious surface, and to a lesser degree also increased R^2 values for cropland. These results show the importance of using the MODIS time-series data for the sub-pixel LC mapping.

Fig. 5a-c shows the R^2 values derived for each individual image using MODIS-NDVI, MODIS bands 1 and 2, MODIS bands 1, 2, and 6, and MODIS all-band combination as inputs. The performance of sub-pixel tree canopy estimation varied substantially when individual MODIS images (i.e., DOY) were used. The time-period between DOY 185 (early-July) to 241 (late-August) appeared to be most useful; because leaves on

the plants and deciduous trees have fully grown and tree canopy density has reached the highest during this time period. For impervious surfaces, images obtained between DOY 201 (mid July) to 249 (early-September) generated the best performance. This may also be explained by vegetation-related dynamics, because impervious surface can be best detected when other natural land surfaces are fully or partially covered by vegetation. For sub-pixel mapping of cropland, there were two peaks of R^2 occurred around DOY 113 (late-April) and 161 (early-June). The timing of the first peak corresponded well with the growing season of winter wheat. The high R^2 value thus may suggest high potential of wheat identification using MODIS images obtained around DOY 113. The second peak can be linked to the phenological development of the major summer crops such as corn and soybean. These summer crop types just started their green up around early-June, thus they can be successfully detected using MODIS surface reflectance data. The performance of MODIS images between DOY 175 to DOY 250 dropped substantially, but increased again after DOY 250 (late-September), which is related to the start of mature-harvest stages for some summer crops.

We further examined the temporal composition of three MODIS images from DOY 185, 217, and 113 for the sub-pixel classification, because these three individual images performed best for tree canopy, impervious surface, and cropland, respectively. The MODIS surface reflectance bands 1–7 were used in the temporal composition. This approach generated R^2 values of 0.55, 0.66, and 0.30 for three cover types, respectively. These values were very similar to those obtained from the entire time-series data. This suggested that it is possible to reduce the input data dimension and increase the computation efficiency, if appropriate individual images are selected from the MODIS data.

V. CONCLUSIONS

This research examined sub-pixel classification of tree canopy, impervious surface, and cropland in the Laurentian GLB. The accuracy assessments were conducted using NLCD-2001 as reference data. Both entire-region and ecoregion-stratified training approaches were examined. Ecoregion stratification did not improve the sub-pixel classification performance. There were large variations of classification accuracies across different ecoregions, mainly due to high variations in LC patterns. Different MODIS data products were examined for the sub-pixel classification. Overall, the MODIS all-band combination achieved the best sub-pixel performance for impervious surface and cropland mapping. The combination of MODIS bands 1 and 2 yielded relatively high accuracy for tree canopy with a lower number of input features, thus it has the advantage in computational efficiency. The accuracies of sub-pixel classification were much improved when the results were aggregated from 250 m to a coarse spatial resolution of 500 m. The sub-pixel classification performances were also examined using individual images corresponding to different DOY. The best

results were achieved at Julian days 185 (early-July), 217 (early-August), and 113 (late-April) for tree canopy, impervious surface, and cropland, respectively. The importance of these DOY images can be attributed to dynamics of vegetation and major crop types.

REFERENCES

- [1] R. A. Houghton, "The worldwide extent of land-use change," *Bioscience*, vol. 44, pp. 305-313, May 1994.
- [2] R. A. Houghton, "Revised estimates of the annual net flux of carbon to the atmosphere from changes in land use and land management 1850-2000," *Tellus B* 55, pp. 378-390, 2003.
- [3] E. Matthews, "Global vegetation and land-use - new high-resolution data-bases for climate studies," *Journal of Climate and Applied Meteorology*, vol. 22, pp. 474-487, 1983.
- [4] M. A. Friedl, D. K. McIver, J. C. F. Hodges, X. Y. Zhang, D. Muchoney, A. H. Strahler, C. E. Woodcock, S. Gopal, A. Schneider, A. Cooper, A. Baccini, F. Gao, and C. Schaaf, "Global land cover mapping from MODIS: algorithms and early results," *Remote Sensing of Environment*, vol. 83, pp. 287-302, Nov 2002.
- [5] M. C. Hansen, R. S. DeFries, J. R. G. Townshend, M. Carroll, C. DiMiceli, and R. A. Sohlberg, "Global percent tree cover at a spatial resolution of 500 meters: first results of the MODIS vegetation continuous fields algorithm," *Earth Interactions*, vol. 7, pp. 1-15, 2003.
- [6] C. O. Justice, E. Vermote, J. R. G. Townshend, R. Defries, D. P. Roy, D. K. Hall, V. V. Salomonson, J. L. Privette, G. Riggs, A. Strahler, W. Lucht, R. B. Myneni, Y. Knyazikhin, S. W. Running, R. R. Nemani, Z. M. Wan, A. R. Huete, W. van Leeuwen, R. E. Wolfe, L. Giglio, J. P. Muller, P. Lewis, and M. J. Barnsley, "The Moderate Resolution Imaging Spectroradiometer (MODIS): land remote sensing for global change research," *Ieee Transactions on Geoscience and Remote Sensing*, vol. 36, pp. 1228-1249, Jul 1998.
- [7] D. P. Roy, P. E. Lewis, and C. O. Justice, "Burned area mapping using multi-temporal moderate spatial resolution data - a bi-directional reflectance model-based expectation approach," *Remote Sensing of Environment*, vol. 83, pp. 263-286, Nov 2002.
- [8] J. F. Knight, R. S. Lunetta, J. Ediriwickrema, and S. Khorram, "Regional scale land cover characterization using MODIS-NDVI 250 m multi-temporal imagery: A phenology-based approach," *Giscience & Remote Sensing*, vol. 43, pp. 1-23, Jan-Mar 2006.
- [9] R. S. Lunetta, J. F. Knight, J. Ediriwickrema, J. G. Lyon, and L. D. Worthy, "Land-cover change detection using multi-temporal MODIS NDVI data," *Remote Sensing of Environment*, vol. 105, pp. 142-154, Nov 2006.
- [10] X. Zhan, R. A. Sohlberg, J. R. G. Townshend, C. DiMiceli, M. L. Carroll, J. C. Eastman, M. C. Hansen, and R. S. DeFries, "Detection of land cover changes using MODIS 250 m data," *Remote Sensing of Environment*, vol. 83, pp. 336-350, Nov 2002.
- [11] T. R. Loveland, B. C. Reed, J. F. Brown, D. O. Ohlen, Z. Zhu, L. Yang, and J. W. Merchant, "Development of a global land cover characteristics database and IGBP DIScover from 1 km AVHRR data," *International Journal of Remote Sensing*, vol. 21, pp. 1303-1330, Apr 2000.
- [12] J. H. Smith, S. V. Stehman, J. D. Wickham, and L. M. Yang, "Effects of landscape characteristics on land-cover class accuracy," *Remote Sensing of Environment*, vol. 84, pp. 342-349, Mar 2003.
- [13] G. M. Foody, "Status of land cover classification accuracy assessment," *Remote Sensing of Environment*, vol. 80, pp. 185-201, Apr 2002.
- [14] D. B. Lobell and G. P. Asner, "Cropland distributions from temporal unmixing of MODIS data," *Remote Sensing of Environment*, vol. 93, pp. 412-422, Nov 2004.
- [15] P. M. Atkinson, M. E. J. Cutler, and H. Lewis, "Mapping sub-pixel proportional land cover with AVHRR imagery," *International Journal of Remote Sensing*, vol. 18, pp. 917-935, 1997.
- [16] R. S. DeFries, J. R. G. Townshend, and M. C. Hansen, "Continuous fields of vegetation characteristics at the global scale at 1-km resolution," *Journal of Geophysical Research-Atmospheres*, vol. 104, pp. 16911-16923, Jul 1999.
- [17] M. C. Hansen, R. S. DeFries, J. R. G. Townshend, R. Sohlberg, C. DiMiceli, and M. Carroll, "Towards an operational MODIS continuous field of percent tree cover algorithm: examples using AVHRR and MODIS data," *Remote Sensing of Environment*, vol. 83, pp. 303-319, Nov 2002.
- [18] C. G. Homer, R. D. Ramsey, T. C. Edwards, and A. Falconer, "Landscape cover-type modeling using a multi-scene thematic mapper mosaic," *Photogrammetric Engineering and Remote Sensing*, vol. 63, pp. 59-67, Jan 1997.
- [19] J. Chang, M. C. Hansen, K. Pittman, M. Carroll, and C. DiMiceli, "Corn and soybean mapping in the united states using MODN time-series data sets," *Agronomy Journal*, vol. 99, pp. 1654-1664, Nov-Dec 2007.
- [20] C. Hüttich, U. Gessner, M. Herold, B. J. Strohbach, M. Schmidt, M. Keil, and S. Dech, "On the Suitability of MODIS Time Series Metrics to Map Vegetation Types in Dry Savanna Ecosystems: A Case Study in the Kalahari of NE Namibia," *Remote Sensing*, vol. 1, pp. 620-643, Sept. 2009.
- [21] C. M. Bishop, *Pattern recognition and machine learning*: Springer, 2006.
- [22] B. Tan, C. E. Woodcock, J. Hu, P. Zhang, M. Ozdogan, D. Huang, W. Yang, Y. Knyazikhin, and R. B. Myneni, "The impact of gridding artifacts on the local spatial properties of MODIS data: Implications for validation, compositing, and band-to-band registration across resolutions," *Remote Sensing of Environment*, vol. 105, pp. 98-114, Nov 2006.
- [23] P. T. Wolter, C. A. Johnston, and G. J. Niemi, "Land Use Land Cover change in the US Great Lakes basin 1992 to 2001," *Journal of Great Lakes Research*, vol. 32, pp. 607-628, 2006.
- [24] D. L. Erickson, "Rural land-use and land-cover change - implications for local -planning in the river raisin watershed," *Land Use Policy*, vol. 12, pp. 223-236, Jul 1995.
- [25] B. Crosbie and P. Chow-Fraser, "Percentage land use in the watershed determines the water and sediment quality of 22 marshes in the Great Lakes basin," *Canadian Journal of Fisheries and Aquatic Sciences*, vol. 56, pp. 1781-1791, Oct 1999.
- [26] N. E. Detenbeck, S. M. Galatowitsch, J. Atkinson, and H. Ball, "Evaluating perturbations and developing restoration strategies for inland wetlands In the Great Lakes Basin," *Wetlands*, vol. 19, pp. 789-820, Dec 1999.
- [27] C. Homer, C. Q. Huang, L. M. Yang, B. Wylie, and M. Coan, "Development of a 2001 National Land-Cover Database for the United States," *Photogrammetric Engineering and Remote Sensing*, vol. 70, pp. 829-840, Jul 2004.
- [28] P. Jonsson and L. Eklundh, "TIMESAT - a program for analyzing time-series of satellite sensor data," *Computers & Geosciences*, vol. 30, pp. 833-845, Oct 2004.
- [29] J. M. Omernik, "Ecoregions of the conterminous united-states," *Annals of the Association of American Geographers*, vol. 77, pp. 118-125, Mar 1987.
- [30] R. Fernandes, R. Fraser, R. Latifovic, J. Cihlar, J. Beaubien, and Y. Du, "Approaches to fractional land cover and continuous field mapping: A comparative assessment over the BOREAS study region," *Remote Sensing of Environment*, vol. 89, pp. 234-251, Jan 2004.
- [31] W. G. Liu and E. Y. Wu, "Comparison of non-linear mixture models: sub-pixel classification," *Remote Sensing of Environment*, vol. 94, pp. 145-154, 2005.
- [32] C. Song, "Spectral mixture analysis for subpixel vegetation fractions in the urban environment: How to incorporate endmember variability?" *Remote Sensing of Environment*, vol. 95, pp. 248-263, 2005.
- [33] G. E. Heilman, J. R. Stritholt, N. C. Slosser, and D. A. Dellasala, "Forest fragmentation of the conterminous United States: Assessing forest intactness through road density and spatial characteristics," *Bioscience*, vol. 52, pp. 411-422, May 2002.
- [34] C. S. Wu and A. T. Murray, "Estimating impervious surface distribution by spectral mixture analysis," *Remote Sensing of Environment*, vol. 84, pp.493-505, 2003.
- [35] S. J. Goetz, R. K. Wright, A. J. Smith, E. Zinecker, and E. Schaub, "IKONOS imagery for resource management: Tree cover, impervious surfaces, and riparian buffer analyses in the mid-Atlantic region," *Remote Sensing of Environment*, vol. 88, pp. 195-208, Nov 2003.
- [36] Q. H. Weng, X. F. Hu, and D. S. Lu, "Extracting impervious surfaces from medium spatial resolution multispectral and hyperspectral imagery: a comparison," *International Journal of Remote Sensing*, vol. 29, pp. 3209-3232, 2008.

- [37] R.E. Wolfe, D.P. Roy, E.F. Vermote, "The MODIS land data storage, gridding and compositing methodology: Level 2 Grid," *IEEE Transactions on Geoscience and Remote Sensing*, 36, pp. 1324-1338, 1998.
- [38] R.E. Wolfe, M. Nishihama, A.J. Fleig, J.A. Kuyper, D.P. Roy, J.C. Storey, "Achieving sub-pixel geolocation accuracy in support of MODIS land science," *Remote Sensing of Environment*, 83, 31-49, 2002.

Tables

TABLE I. All tested sub-pixel classification scenarios for tree canopy, impervious surface, and cropland across the GLB.

TABLE II. MODIS-NDVI sub-pixel classification results for individual ecoregions. Sub-pixel estimations derived from 250 m MODIS-NDVI (2001) were compared with proportions derived from NLCD-2001.

TABLE III. Comparison of sub-pixel classification results using MODIS-NDVI and MODIS surface reflectance bands. Sub-pixel estimations derived from MODIS-NDVI and surface reflectance bands (2001) were compared with the land cover proportions derived from the NLCD-2001.

TABLE IV. Comparison of sub-pixel classification results using MODIS-NDVI and MODIS surface reflectance bands. Sub-pixel estimations derived from MODIS-NDVI and surface reflectance bands (2001) were compared with the land cover proportions derived from the NLCD-2001. Sub-pixel cover type proportions were aggregated to 500 m for comparison.

TABLE V. GLB accuracy assessment statistics (250 m) using the different MODIS data products as inputs. Reported are the highest R^2 values derived using individual images (a) and the entire MODIS time-series data (b). The corresponding DOY (97–273) for each R^2 value are also reported.

Figures

Fig. 1. Ecological regions across the United States portion of the Great Lakes Basin based on a modified Omernik (1987) classification system. The ecoregion boundaries were used to stratify the MODIS-NDVI sub-pixel classifications.

Fig. 2. Comparison of entire-region and ecoregion-stratified image classification approaches for tree canopy (a), impervious surfaces (b), and cropland (c).

Fig. 3. Scatter plots for three sub-pixel cover types at 250 m and 500 m resolutions. MODIS all-band (1–7) combination was used as the input for the sub-pixel estimation.

Fig. 4. The sub-pixel proportional maps for tree canopy (b), impervious surfaces (c), and cropland (d). MODIS all-band (1–7) combination was used to support the analysis.

Fig. 5 (a-c). The Pearson R² values derived for each individual image composite using MODIS-NDVI, MODIS bands 1 and 2, MODIS bands 1, 2, and 6, and MODIS bands 1–7 for tree canopy (a), impervious surfaces (b), and cropland (c).

TABLE I. All tested sub-pixel classification scenarios for tree canopy, impervious surface, and cropland across the GLB.

Sub-pixel classification	Input dataset
Entire GLB approach versus ecoregion stratified approach	MODIS-NDVI (16-day composite)
Comparison of different input feature/band combinations (entire GLB approach)	MODIS-NDVI (16-day composite)
	MODIS surface reflectance bands 1,2 (8-day composite)
	MODIS surface reflectance three-band combination (8-day composite)
	MODIS surface reflectance seven-band combination (8-day composite)
Comparison of individual image (DOY) and time-series data (entire GLB approach)	MODIS-NDVI (16-day composite)
	MODIS surface reflectance bands 1,2 (8-day composite)
	MODIS surface reflectance three-band combination (8-day composite)
	MODIS surface reflectance seven-band combination (8-day composite)

TABLE II. MODIS-NDVI sub-pixel classification results for individual ecoregions. Sub-pixel estimations derived from 250 m MODIS-NDVI (2001) were compared with proportions derived from NLCD-2001.

	Tree Canopy		Impervious Surfaces		Cropland	
	RMSE	R^2	RMSE	R^2	RMSE	R^2
Ecoregion 1	0.26	0.21	0.19	0.39	0.32	0.07*
Ecoregion 2	0.25	0.23	0.15	0.19	0.33	0.05*
Ecoregion 3	0.23	0.33	0.16	0.51	0.34	0.10
Ecoregion 4	0.21	0.19	0.17	0.41	0.28	0.21
Ecoregion 5	0.20	0.42	0.18	0.55	0.28	0.21
Ecoregion 6	0.20	0.43	0.19	0.51	0.28	0.23
Ecoregion 7	0.20	0.37	0.11	0.25	0.25	0.10
Ecoregion 8	0.21	0.50	0.12	0.28	0.30	0.14
Ecoregion 9	0.18	0.38	0.15	0.37	0.31	0.05*
Ecoregion 10	0.19	0.37	0.22	0.61	0.30	0.10
All	0.20	0.50	0.18	0.51	0.29	0.24

* Statistically insignificant ($p = 0.01$)
 RMSE (root-mean-square-error)

TABLE III. Comparison of sub-pixel classification results using MODIS-NDVI and MODIS surface reflectance bands. Sub-pixel estimations derived from MODIS-NDVI and surface reflectance bands (2001) were compared with the land cover proportions derived from the NLCD-2001.

Resolution (250 m)	Tree Canopy		Impervious Surfaces		Cropland	
	RMSE	R^2	RMSE	R^2	RMSE	R^2
NDVI	0.20	0.50	0.18	0.51	0.29	0.24
2 MODIS Bands (1,2)	0.19	0.56	0.17	0.57	0.27	0.28
3 MODIS Bands (1,2,6)	0.19	0.57	0.16	0.59	0.26	0.30
7 MODIS Bands (1-7)	0.19	0.57	0.15	0.63	0.26	0.30

All R^2 values are statistically significant ($p = 0.01$)

TABLE IV. Comparison of sub-pixel classification results using MODIS-NDVI and MODIS surface reflectance bands. Sub-pixel estimations derived from MODIS-NDVI and surface reflectance bands (2001) were compared with the land cover proportions derived from the NLCD-2001. Sub-pixel land cover proportions were aggregated to 500 m for comparison.

Resolution (500 m)	Tree Canopy		Impervious Surfaces		Cropland	
	RMSE	R^2	RMSE	R^2	RMSE	R^2
NDVI	0.16	0.68	0.17	0.58	0.22	0.49
2 MODIS Bands (1,2)	0.15	0.75	0.16	0.60	0.18	0.56
3 MODIS Bands (1,2,6)	0.14	0.76	0.14	0.65	0.18	0.59
7 MODIS Bands (1-7)	0.14	0.76	0.13	0.68	0.18	0.59

All R^2 values are statistically significant ($p = 0.01$)

TABLE V. GLB accuracy assessment statistics (250 m) using the different MODIS data products as inputs. Reported are the highest R^2 values derived using individual images (a) and the entire MODIS time-series data (b). The corresponding DOY (97–273) for each R^2 value are also reported.

(a) Individual Images	MODIS Products/Band Combinations			
	NDVI	bands 1,2	bands 1,2,6	bands 1–7
Tree Canopy	0.40 (193)	0.38 (185)	0.44 (185)	0.46 (185)
Impervious Surfaces	0.45 (209)	0.47 (217)	0.48 (217)	0.60 (217)
Cropland	0.21 (145)	0.21 (113)	0.22 (113)	0.26 (113)

All R^2 values are statistically significant ($p = 0.01$)

(b) All Images	MODIS Products/Band Combinations			
	NDVI	bands 1,2	bands 1,2,6	bands 1–7
Tree Canopy	0.50	0.56	0.57	0.56
Impervious Surfaces	0.51	0.57	0.59	0.63
Cropland	0.24	0.28	0.30	0.30

All R^2 values are statistically significant ($p = 0.01$)

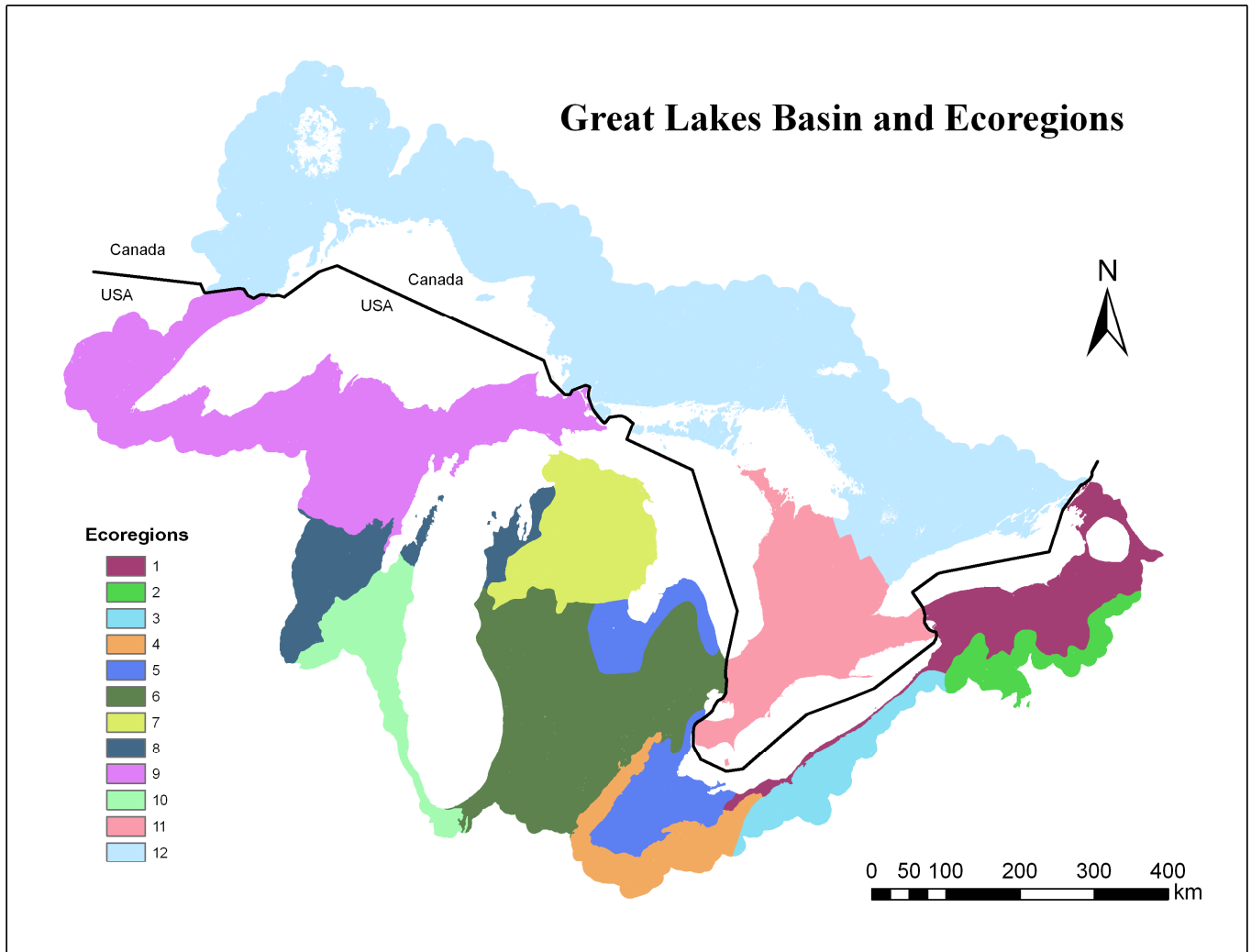


Fig. 1. Ecological regions across the United States portion of the Great Lakes Basin based on a modified Omernik (1987) classification system. The ecoregion boundaries were used to stratify the MODIS-NDVI sub-pixel classifications.

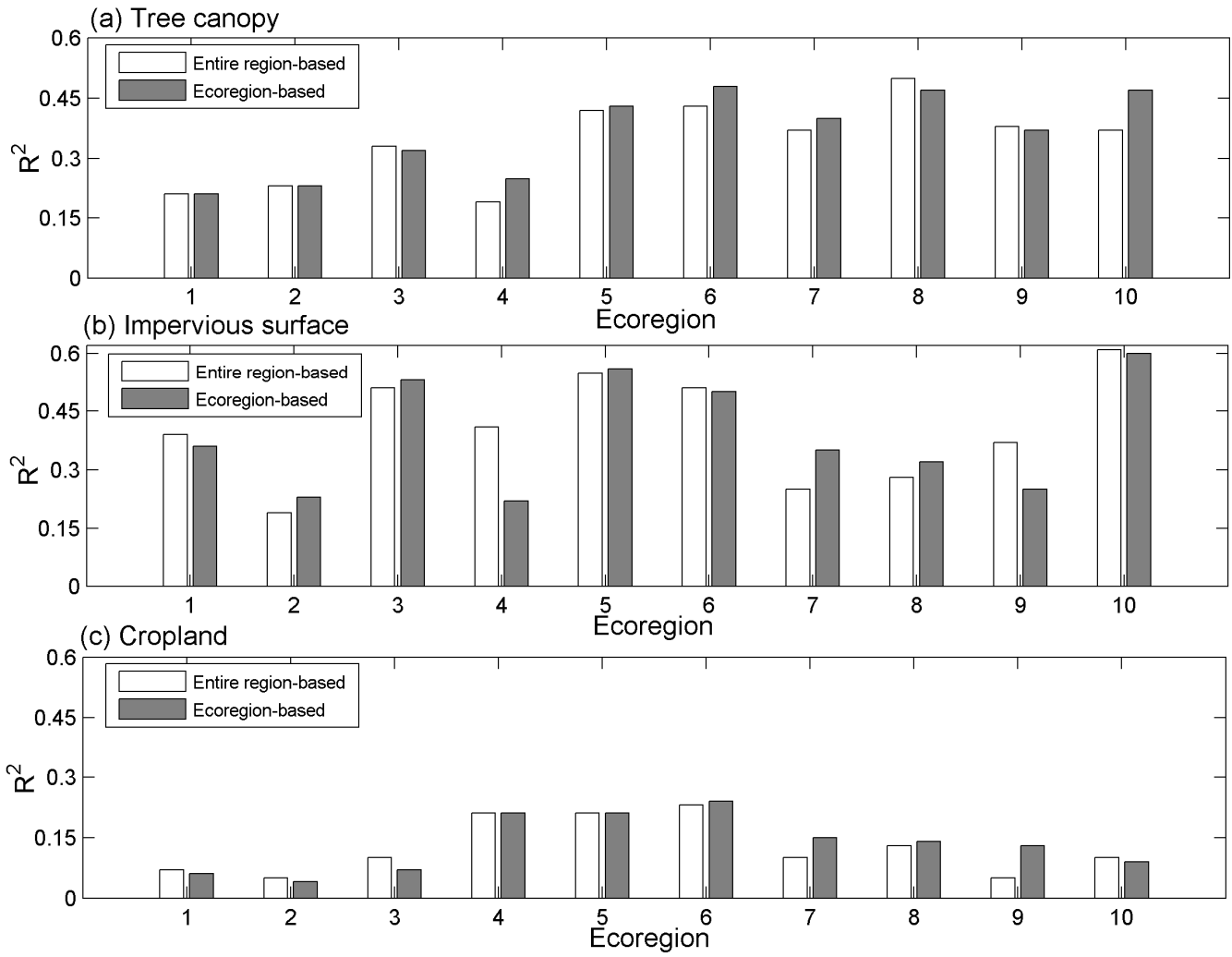


Fig. 2. Comparison of entire-region and ecoregion-stratified image classification approaches for tree canopy (a), impervious surfaces (b), and cropland (c).

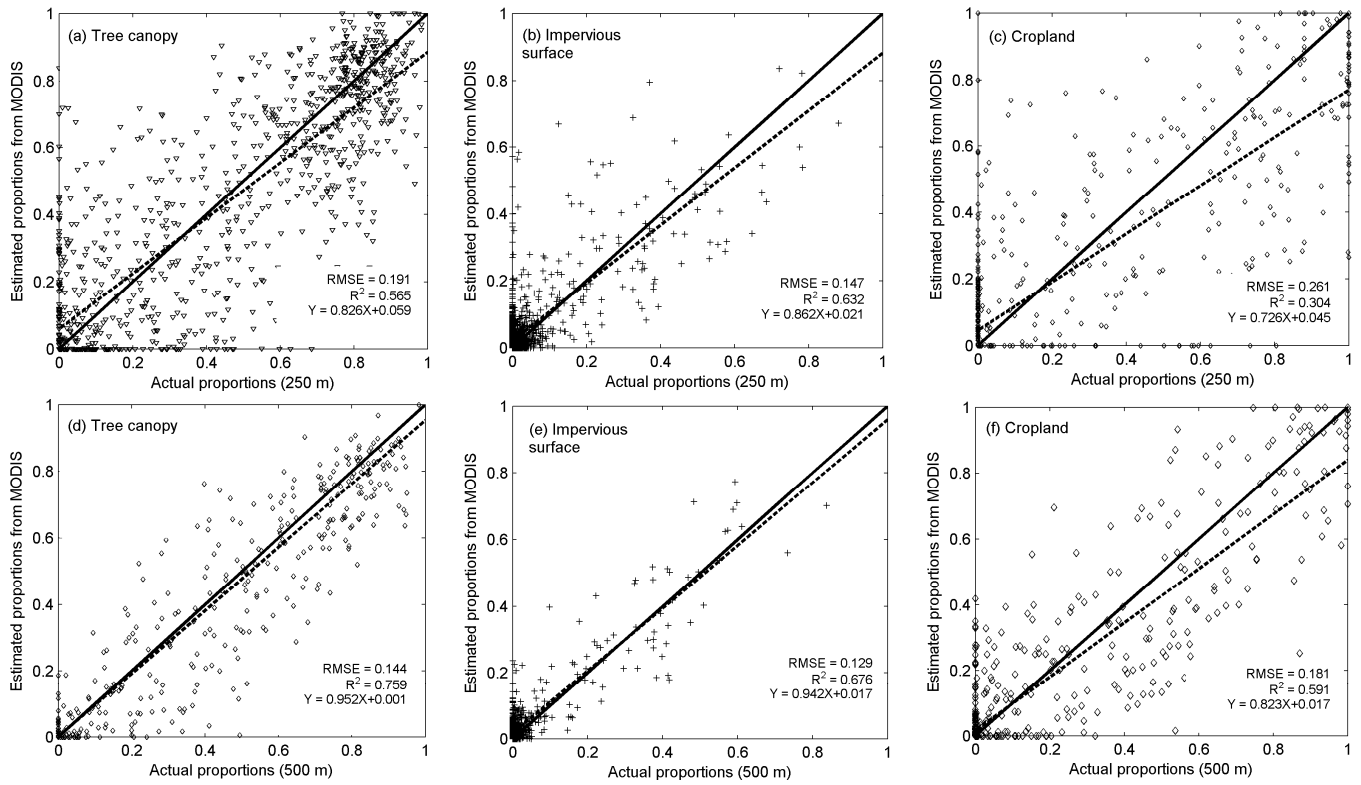


Fig. 3. The scatter plots for three sub-pixel cover types at 250 m and 500 m resolutions. MODIS all-band (1–7) combination was used as the input for the sub-pixel estimation.

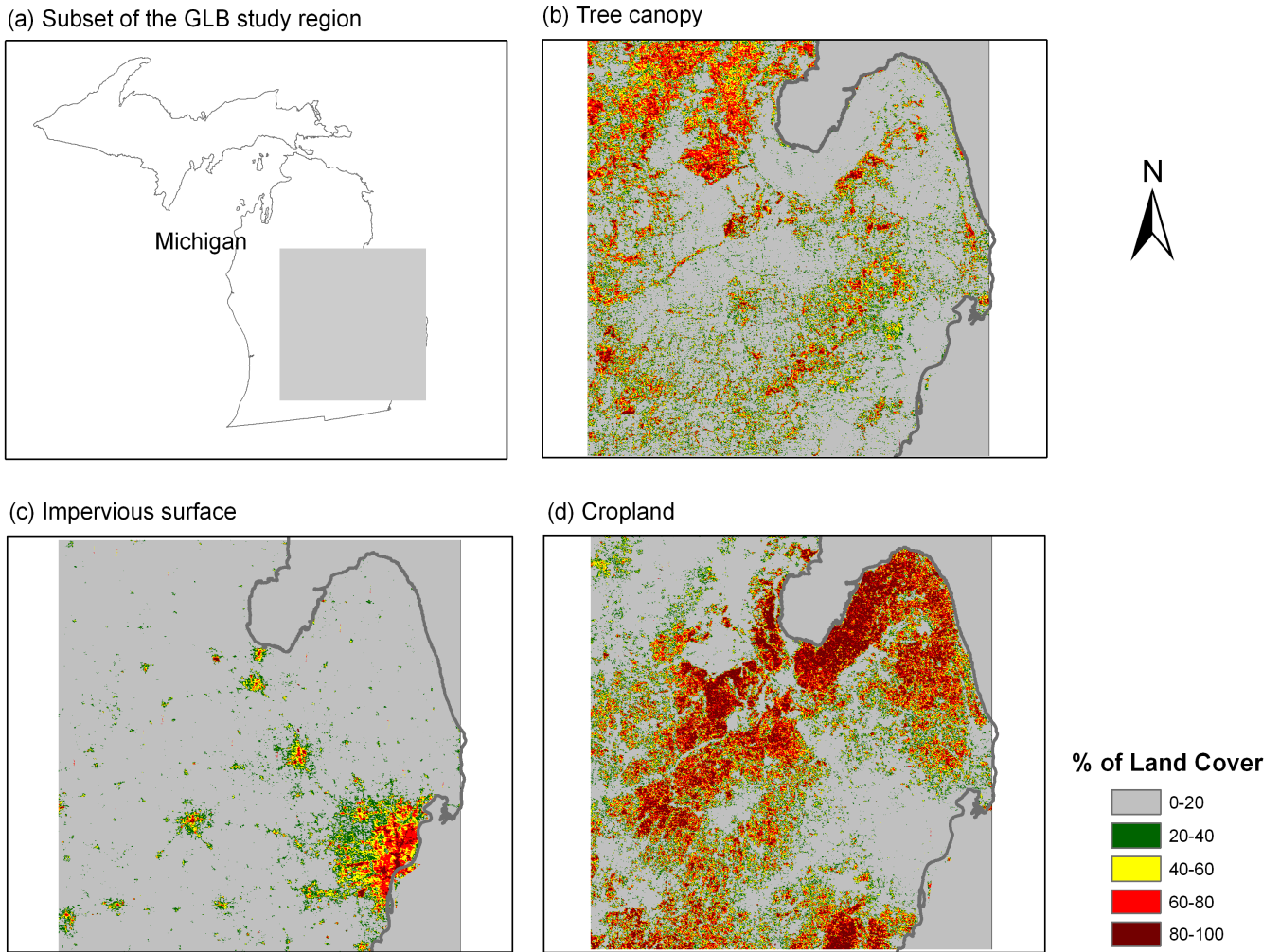


Fig. 4. The sub-pixel proportional maps for tree canopy (b), impervious surfaces (c), and cropland (d). MODIS all-band (1–7) combination was used to support the analysis.

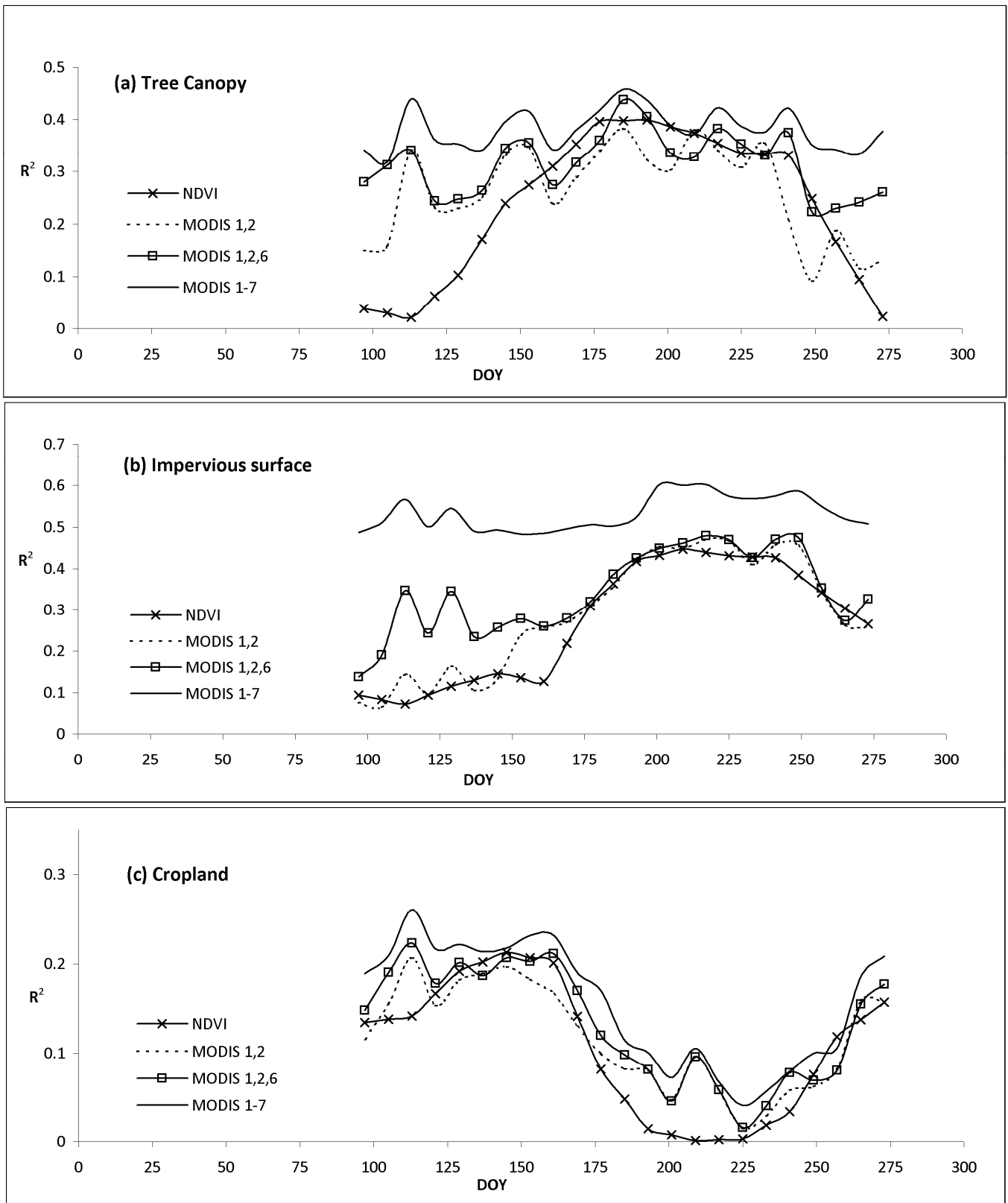


Fig. 5 (a-c). The Pearson R² values derived for each individual image composite using MODIS-NDVI, MODIS bands 1 and 2, MODIS bands 1, 2, 6, and MODIS bands 1–7 for tree canopy (a), impervious surfaces (b), and cropland (c).